ICES Journal of Marine Science, 2025, Vol. 82, Issue 1, fsaf005
https://doi.org/10.1093/icesjms/fsaf005
Received: 30 September 2024; **revised:** 31 December 2024; **accepted:** 7 January 2025
Original Article

Krill swarm biomass, energetic density, and species composition drive humpback whale distribution in the Northern California Current

Rachel L. Kaplan [1,2,*], Kim S. Bernard [1], Solène Derville [3], Jennifer L. Fisher [4], Elizabeth M. Phillips [5], Elizabeth A. Daly [6], Joseph D. Warren [7], L.G. Torres [2]

[1]College of Earth, Ocean, and Atmospheric Sciences, Oregon State University, 104 Ocean Admin Bldg, Corvallis, OR 97331, United States
[2]Geospatial Ecology of Marine Megafauna Lab, Marine Mammal Institute, Department of Fisheries, Wildlife and Conservation Sciences, Oregon State University, 2030 SE Marine Science Drive, Newport, OR 97365, United States
[3]UMR ENTROPIE (UR-IRD-IFREMER-CNRS-UNC), Noumea 98800, New Caledonia
[4]NOAA-Fisheries, NWFSC, Hatfield Marine Science Center, 2030 SE Marine Science Dr, Newport, OR 97365, United States
[5]Fishery Resource Analysis and Monitoring Division, Northwest Fisheries Science Center, National Marine Fisheries Service, National Oceanic and Atmospheric Administration, 2725 Montlake Blvd E., Seattle, WA 98112, United States
[6]Cooperative Institute for Marine Ecosystem and Resources Studies, Oregon State University, Newport, OR 97365, United States
[7]School of Marine and Atmospheric Sciences, Stony Brook University, Southampton, NY 11968, United States

*Corresponding author. Rachel L.Kaplan, College of Earth, Ocean, and Atmospheric Sciences, Oregon State University, 104 Ocean Admin Bldg, Corvallis, OR 97331, United States. E-mail: kaplarac@oregonstate.edu

Abstract

Prey abundance and quality are dynamic in time and space, impacting predator ecology. We examine variation in species-specific krill quantity and quality as prey for humpback whales in the Northern California Current region, using generalized additive models to assess metrics including biomass and energy density derived from an integrated dataset of concurrent active acoustics, net tows, and marine mammal observations (2018–2022). Overall, prey metrics were positively correlated with humpback whale presence, with increasing trends modified by seasonal (early versus late foraging season) and spatial (continental shelf versus offshore) variation (model deviance explained 36.3%–40.8%). Biomass and energy density had strong positive effects on humpback whale presence, suggesting whales target high-quality swarms that offer more energy per lunge. Elevated *Thysanoessa spinifera* abundance near humpback whales suggests that they target this species, particularly in the late season when they are energetically richer than *Euphausia pacifica*, the region's other abundant krill species. Environmental change may decrease krill abundance and quality, impacting humpback whales' ability to meet energetic requirements and potentially driving changes in their distributions and exposure to anthropogenic threats. Clarifying drivers of humpback whale krill patch selection can improve species distribution models and aid managers in mitigating risk to whales.

Keywords: active acoustics; krill; prey quality; spatial ecology; Northern California Current; humpback whales

Introduction

Krill are an important prey resource across ocean ecosystems (Cotté et al. 2011, Miller et al. 2019, Videsen et al. 2023). Both prey quantity and quality are variable in time and space and influence whether a resource is advantageous to a predator (Spitz et al. 2012, Cade et al. 2022). For large predators like baleen whales, sufficient prey biomass is essential to meet energetic demands and support activity during nonforaging life history phases, including reproduction (Jönsson 1997). Extreme body size ratios relative to their prey require baleen whales to feed on aggregated patches (Benoit-Bird 2024), such as krill swarms (Brinton 1962). In Antarctica, krill swarm height, packing density, and depth drive patch selection for foraging blue whales (*Balaenoptera musculus*) across spatiotemporal scales (Miller et al. 2019). The depth and density of krill aggregations control blue whale dive depth in Southern California (Goldbogen et al. 2015) and the St. Lawrence River Estuary, and whales maximize net energy gain by balancing travel time to the prey, recovery time after dives, and resource acquisition (Doniol-Valcroze et al. 2011).

The energetic content of krill themselves also shapes whale foraging choices and strategies. In Western Antarctic Peninsula fjords, humpback whales (*Megaptera novengliae*) target larger krill with higher energetic value (Cade et al. 2022). In the California Current System (CCS), blue whales target calorically rich *Thysanoessa spinifera*, although this species is less abundant compared to other krill species (Fiedler et al. 1998, Nickels et al. 2018). Foraging whales may prey-switch, a strategy in which animals target prey based on relative availability and quality (Murdoch 1969). Compared to blue whales, which are obligate krill predators (Fiedler et al. 1998, Mizroch et al. 2009, Fossette et al. 2017), humpback and fin whales (*Balaenoptera physalus)* prey-switch to consume a broader diet including pelagic fish.

Oceanographic processes influence krill quantity and quality across time and space, shaping the preyscape encountered by predators on their foraging grounds (Fleming et al. 2016, Ryan et al. 2022). The CCS is a productive Eastern Boundary Current Upwelling System in the northeast Pacific Ocean off the United States west coast, extending south from

Vancouver Island, British Columbia, to Baja California, Mexico (Checkley and Barth 2009). In the Northern California Current (NCC), from Cape Mendocino, California, to Vancouver Island, krill are essential prey for taxa including baleen whales (humpback, blue, and fin whales; Fiedler et al. 1998, Mizroch et al. 2009). Two dominant species, *Euphausia pacifica* and *T. spinifera* (hereafter "krill"), together comprise >95% of the krill community (T. Shaw and J. Fisher personal communication). *Thysanoessa spinifera* are more lipid-rich than *E. pacifica* (Fisher et al. 2020) and are the preferred prey of blue whales (Fiedler et al. 1998). However, the caloric content of both krill species may be impacted by life history traits and dynamic primary productivity processes that vary in space and time (Färber-Lorda et al. 2009, Price et al. 2024). Further research is needed to explain how energy density varies relative to krill body size, sex, reproductive stage, species, and season, and how this bioenergetic variability impacts the NCC marine food web (Price et al. 2024).

Pursuing more energetically dense prey can increase the profitability of a given mouthful and help a whale offset the energy expended to earn it (Chenoweth et al. 2021), particularly the costly hunt for prey on the foraging grounds (Videsen et al. 2023). Humpback whales migrate to NCC foraging grounds annually from low-latitude breeding grounds. As generalist predators, they target krill and prey-switch to fish in response to basin-scale climate and environmental processes (Fleming et al. 2016, Fossette et al. 2017, Santora et al. 2020). In this study, we examine fine-scale (5 km; Kaplan et al. 2024) variation in krill quantity and quality as prey for humpback whales on the NCC foraging grounds, comparing the early foraging season (March–June) that follows the initiation of upwelling (Checkley and Barth 2009) with the late foraging season (July–November) when upwelling peaks and subsides (Jorgensen et al. 2024). We analyze metrics of krill swarm biomass, energetic density, and species composition in relation to humpback whale distribution. We hypothesize that humpback whales are observed in association with higher biomass swarms and/or those with higher energetic densities and increased *T. spinifera* composition.

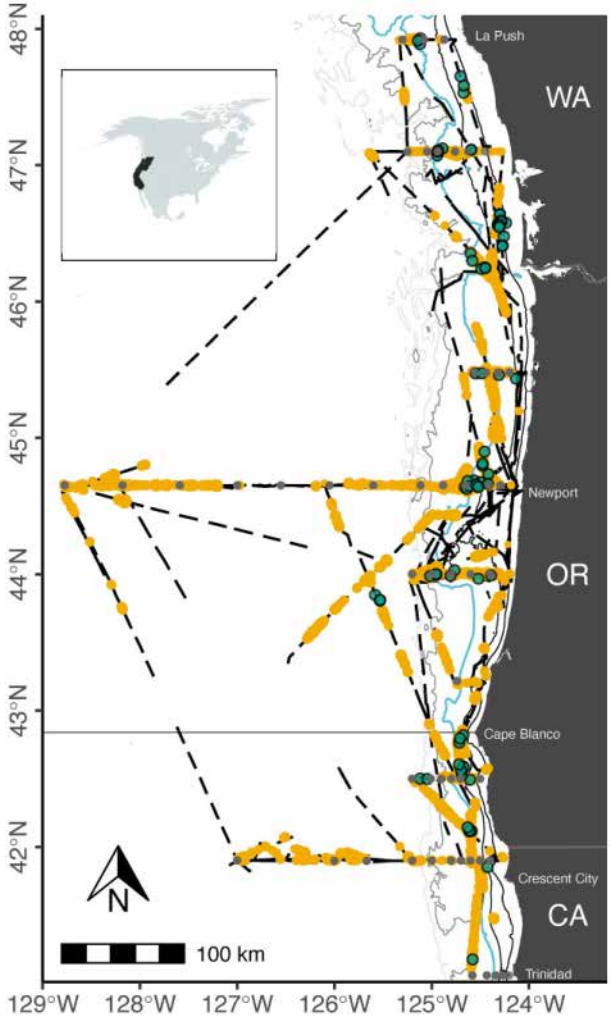

Figure 1. Map of study area illustrating concurrent marine mammal observation and echosounder data (dashed black lines). Detected krill swarms (orange) are scaled by biomass (kg). Gray dots: bongo net tows; green dots: humpback whale groups. Isobaths (50, 100, 1000, and 1500 m) are represented by gray lines (deeper isobaths are shown in progressively lighter colors), and the 200 m isobath designating the shelf break is blue-green.

Methods

Survey background

Since 2018, the National Oceanic and Atmospheric Administration's (NOAA) Northern California Current Ecosystem Surveys (hereafter, "NCC surveys") have sampled hydrographic transects and collected underway marine mammal observations between La Push, Washington, and Crescent City, Trinidad, or San Francisco, California, aboard the NOAA Ship "Bell M. Shimada" approximately three times per year in the winter, spring, and fall (February, May, and September). We integrated active acoustic and net sampling data to characterize the quantity and quality of krill and matched these data with concurrent observations of humpback whales (Fig. 1). Our study focuses on the NCC from Cape Mendocino to La Push, which was sampled during eight surveys between 2018 and 2022 (Table 1).

Krill sampling for community composition, lengths, and modeled distributions

At long-term, established oceanographic stations (Fig. 1), the zooplankton community was sampled at nighttime and dusk by towing a bongo net with a 0.6 m mouth diameter and 335 μm mesh obliquely to 100 meters depth (Table 1). Samples were preserved in 5% buffered formalin solution and brought ashore for later analysis. In the laboratory, samples were split using a Folsom splitter, and krill were identified to species and life history stage (juvenile, immature adult, mature female, and mature male), and standard lengths were measured (reported as standard length 2, from the anterior of the eye to the end of the sixth abdominal segment; Mauchline 1980). Juveniles were defined as <10 mm, and mature adults were >10 mm with a petasma (male), thelycum (female), or no external reproductive features (immature adults). These data allowed us to characterize the lengths, sex, stage, and proportion of *E. pacifica* and *T. spinifera* at every sampling station.

We modeled the proportion of *T. spinifera* (and reciprocally, *E. pacifica*) to inform species-specific distributions throughout the study region, using a Generalized Additive Model (GAM) ("Distribution *T. spinifera*") fitted with a beta distribution (suitable for data values between 0 and 1) and a logit

Table 1. Concurrent active acoustic and whale observation efforts (km and days) per survey, and krill swarms, bongo net tows, caloric samples, and humpback whale groups included in models

Year	Month	Observation effort (km)	Observation effort (days)	Humpback whale groups	Bongo samples	Krill swarms	Caloric samples
2018	February	320.0	6		2		
	March				1		
	May	574.8	8	6	17	137	2
	June						2
	September	776.2	7	2	18	144	
2019	April				1		2
	May	660.2	8		3	187	8
	June						4
	September	869.5	9	6	19	250	
2020	March				6		
	June						9
	September	806.1	8	27	18	121	
2021	March						7
	April						8
	May	946.9	3		10	52	10
	June						9
	July						4
	August						2
	November						2
2022	March						5
	April						23
	May	909.3	8	33	18	199	147
	June						1
	July						1
	September	401.5	3	2	9	2	88

Note caloric samples were sometimes collected during surveys that did not include observation effort.

link function. Explanatory variables included distance from the continental shelf break (designated by the 200 m isobath) with unspecified basis size, latitude with a basis size of 5 (to capture any latitudinal distribution variability), season (fall, winter, and spring), and year (2018–2022; Table S2). Smooth functions were fit to the continuous data using penalized thin plate regression splines, and nonsignificant variables were penalized to zero (Marra and Wood 2011). All statistical analyses were conducted in R 4.3.1 (R Core Team 2024).

Krill energetic data

During the May and September 2022 NCC surveys, krill (up to 30 individuals/tow) were collected from bongo net tows and frozen individually at −80°C in cryovials (Table 1). Additional samples were collected opportunistically within the study region between 2018 and 2022 and frozen in seawater at −80°C as whole samples in clean plastic bags (Table 1).

In the lab, individual krill were thawed, gently blotted with a Kimwipe, weighed on a microbalance to obtain wet weights, and placed in a desiccating oven at 60°C for 48–72 hours, after which dry weights were recorded. Dried samples were ground into homogenous powder and pressed into pellets. We assessed the caloric content of individual krill ($n = 153$) when possible, adding known quantities of benzoic acid (C_6H_5COOH) to reach the minimum pellet weight for analysis (0.025 g). When krill were too small to be analyzed singly, we grouped 2–3 individuals by species, oceanographic station, stage, sex, reproductive status (with or without attached spermatophores), and length ($n = 181$ grouped samples) to meet the minimum pellet weight. The caloric content of each pellet was quantified using a semi-micro bomb calorimeter (Model 6725, Parr Instruments) and reported in kilojoules per gram wet weight (kJ g^{-1} WW). Due to sampling constraints, krill samples were available during different months and years of our study. We grouped samples temporally into "early" (March–June) and "late" (July–November) seasons to examine relationships broadly across seasons and years. Outlier detection and removal were performed on the species- and season-specific krill caloric data (groups: early season *E. pacifica*, late season *E. pacifica*, early season *T. spinifera*, late season *T. spinifera*) by omitting values outside 1.5 times each group's interquartile range (nine total samples omitted).

Acoustic data and swarm metrics

Active acoustic data were collected using hull-mounted, downward-looking, narrow-band split-beam echosounders (2018 Simrad EK60; 2019–2022 Simrad EK80) operating at multiple frequencies (18, 38, 70, 120, and 200 kHz) during NCC surveys (Table S1; Fig. S1). Data were recorded from the surface to 750 or 1000 m using a 1.024 ms narrow-band pulse at rates between 1 ping per second and 1 ping per 8 seconds, depending on bottom depth.

Complete acoustic data processing methods are available in Kaplan et al. (2024). Briefly, data collected during daytime (sunrise to one hour before sunset) and at survey speeds greater than 5 kt were processed in Echoview 13.1 to calculate the mean volume backscattering strength (MVBS or Sv, dB re 1 m^{-1}) attributable to krill through decibel (dB) differencing, using a range of 10–16.3 dB in the 120 and 38 kHz data (Phillips et al. 2022). Frequency selection for dB differencing can impact the backscatter identified as krill and resulting biomass estimates (Jarvis et al. 2010), and we selected this frequency pair and range for comparability with other efforts in the region (e.g. Phillips et al. 2022, Dorman et al. 2023). We used Echoview's school detection module to identify swarms

from the dB-differenced data based on the following parameters, tuned to fit the dimensions of observed swarms: minimum total school height = 2 m, minimum candidate length = 5 m, minimum candidate height = 2 m, maximum vertical linking distance = 10 m, maximum horizontal linking distance = 52 m, and minimum total school length = 5 m. Descriptors of each swarm were exported, including length (m), thickness (m), MVBS, and NASC (Nautical Area Scattering Coefficient; m^2 nmi^{-2}). As the frequency responses of *E. pacifica* and *T. spinifera* overlap, and NASC integrates scattering from all lengths of krill classified using dB differencing, these values represent the combined abundance of both krill species.

The "Distribution *T. spinifera*" model was used to predict the proportion of *T. spinifera* in each identified swarm. This approach applied a model trained on nighttime tow data to daytime acoustic data, and we assume these methods sampled the same populations since krill in this region undergo diel vertical migration that brings them from depth (mean daytime depth distribution 148 m ± 44 m; Phillips et al. 2022) to the surface at night (Brinton 1967, Dorman et al. 2023). We binned data into four "ecoregions" (onshore-north, offshore-north, onshore-south, and offshore-south) to capture spatial and seasonal (fall: September; winter: February–March; spring: April–May) changes in krill body size, which influence biomass. The 200 m isobath designated onshore and offshore regions, and Cape Blanco (42.84°N), an important oceanographic feature in the NCC, served as the latitudinal boundary between north and south (Fig. 1). Subsequently, we applied the target strength model developed in Dorman et al. (2023) to convert MVBS to krill biomass (kg) and used the median species-specific energetic density of krill sampled in the early and late foraging season to estimate swarm energetic density. See supplementary materials for full methods and equations.

Whale distribution data

Marine mammal observers aboard NCC surveys recorded whale detections and collected data enabling calculation of perpendicular distances between each whale group and the ship's trackline, following a distance sampling protocol (Buckland et al. 2015: see supplementary materials for details). Although these data have previously been analyzed in a distance sampling framework for other purposes (Derville et al. 2022), our study adopted a different approach, focusing on the preyfield as perceived from the whale's perspective. For this analysis, data from humpback whale groups sighted >5 km from the ship's trackline were excluded (methods described in greater detail in Kaplan et al. 2024).

Humpback whale–krill models

Five-kilometer radii circles were drawn around each whale group based on previous findings identifying this as the optimal range for describing humpback whale–krill relationships in the NCC (Kaplan et al. 2024). In addition, we generated points at regular 5 km intervals along the ship's trackline to sample the "background" preyscape (n = 1169 background points) and drew 5 km radius circles around them ("sf" R package; version 1.0–16; Pebesma and Bivand 2023). Krill swarm data (proportion *T. spinifera*, energy density, and biomass) were averaged within 5 km of each humpback whale sighting and background point, and biomass catch per unit effort (hereafter "biomass CPUE"; kg krill/km effort) was calculated by dividing total krill biomass (kg) by effort (km) within each 5 km circle. To compare the krill preyscape in habitats selected by humpback whales versus the background preyscape, prey metrics (proportion *T. spinifera*, swarm energy density, swarm biomass, and biomass CPUE) were analyzed within (i) 5 km of humpback whale sightings and (ii) 5 km of background points. Krill metrics were not normally distributed (Shapiro–Wilk test, $P < .05$), and not all metrics had equal variance (Levene's test, $P < .05$). Therefore, seasonal and spatial relationships were assessed using nonparametric tests on rank-transformed data (Kruskal–Wallis and Type III ANOVA; Conover and Iman 1981, Table 2), and median values are reported.

We assessed relationships between humpback whale presence and five krill swarm metrics: the acoustic abundance proxy NASC, biomass, energetic density, biomass CPUE (a measure of patchiness), and the proportion of *T. spinifera*, which may be a preferred prey item. We formulated five GAMs with humpback whale presence as the response variable and the five krill prey metrics (logged to approximate normal distributions; Table 3): swarm NASC (m^2 nmi^{-2}; "NASC" Model), swarm biomass (kg; "Swarm Biomass" Model), biomass CPUE (kg/km; "Biomass CPUE" Model) as a measure of patchiness, swarm mean energetic density (kilojoules/m^3; "Energetic Density" Model), and the proportion of each swarm comprised of *T. spinifera* (0.0–1.0; "Proportion *T. spinifera*" Model). Pearson's correlation coefficients calculated amongst metrics exceeded 0.5, and most exceeded 0.7 ("corrplot" R package; version 0.92; Wei and Simko 2024, Fig. S2), and therefore explanatory metrics were used in separate models to test each variable independently and minimize collinearity (Dormann et al. 2013). GAMs ("mgcv" R package; version 1.9–1; Wood 2011) predicted humpback whale presence using a binomial distribution with a cloglog link function and restricted maximum likelihood (REML) and penalized thin plate regression splines with a basis size of k = 3 to limit overfitting. Weights were used to balance the total number of background points (n = 1169) with the total number of presence points (n = 76 humpback whale groups, containing 98 total individuals) and account for humpback whale group size (range 1–4 whales/groups). Background point weights (weight = 98 individuals/1169 background points) and presence point weights (increasing with whale group size) were scaled so that the mean of all weights equaled 1, and weights summed to the total number of presence and background points (n = 1245). An interaction term accounted for the effect of season (early versus late foraging season) and location (onshore versus offshore) on the trends fitted between whale presence and prey quality metrics. The survey was included as a random effect to account for variability in broad environmental conditions between years and survey periods, potential variability in acoustic data collection, and other potential observational error.

Results

Spatiotemporal dynamics of krill preyscape quality

The spatial distribution of *T. spinifera* varied significantly with distance from the continental shelf break and among years (deviance explained 39.8%; Table S2). The cross-shelf distribution patterns of the two species opposed one another, with *T. spinifera* concentrated on the continental shelf and at

Table 2. Krill metric test results from rank-transformed ANOVA Type III (A) and Kruskal–Wallis (K)

Metric	Variable	Sum of squares (A)/χ^2 (K)	*F* value/df (K)	*P*	*n*	Test	Data
E. pacifica length	Ecoregion	49.44	3	<.001***	2853	K	2018–2022
	Season	63.552	2	<.001***			
T. spinifera length	Ecoregion	42.073	3	<.001***	631	K	2018–2022
	Season	33.077	2	<.001***			
Krill caloric content	Ecoregion	1.548	2	.461	334	K	2018–2022
Krill caloric content	Species	99 521	14.4479	<.001***	334	A	2018–2022
	Season	783 187	113.6994	<.001***			
	Species:Season	22 019	3.1966	.075			
E. pacifica caloric content	Sex	18	0.0305	.862	86	A	2022
	Spermatophores	3048	5.1233	.026*			
	Sex: Spermatophores	794	1.3354	.251			
T. spinifera caloric content	Sex	137.2	2.4287	.130	34	A	2022
	Spermatophores	1252.3	22.1627	<.001***			
	Sex: Spermatophores	1.5	0.0265	.872			
Swarm Energetic Density	Shelf	6 026 439	14.581	<.001***	2242	A	2018–2022
	Season	7 882 090	19.071	<.001***			
	Shelf: Season	581 120	1.406	.236			
Swarm Biomass	Shelf	19 788 617	48.2489	<.001***	2242	A	2018–2022
	Season	605 039	1.4752	.225			
	Shelf: Season	601 538	1.4667	.226			
Biomass CPUE	Shelf	4440	11.4130	<.001***	76	A	2018–2022
	Season	371	0.9531	.332			
	Shelf: Season	2883	7.4107	<.001***			
Proportion *T. spinifera*	Shelf	157	0.4080	.520	76	A	2018–2022
	Season	2037	5.2962	.025*			
	Shelf: Season	2340	6.0825	.016*			

For each ANOVA term, we report the sum of squares, *F* value, *P* value, and sample size (*n*). For Kruskal–Wallis terms, we report chi-squared (χ^2) and degrees of freedom (df). Swarm energetic density (kilojoules/m^3) and swarm biomass (kg) results describe relationships across the sampled preyscape ($n = 2224$ swarms). Biomass CPUE (catch per unit effort; kg krill/km observation effort) and proportion *T. spinifera* results use data within 5 km of sighted humpback whale groups ($n = 76$). "Ecoregion" denotes the four spatial bins within the study region; "Season" denotes early versus late humpback whale foraging seasons, "Spermatophores" indicates krill reproductive status, and "Shelf" identifies samples as on the continental shelf or offshore.

Table 3. Summary of humpback-krill individual metric models, each calculated as: whale presence ~ prey quality metric × season × location + (1|survey)

Prey quality metric	Dev. exp.	AIC	Effect of prey quality metric by condition				Survey
			Early season—offshore	Late season—offshore	Early season—onshore	Late season—onshore	
Swarm Biomass	40.7%	1509.949	Edf = 1.652 $\chi^2 = 114.74$ $P < .001$	Edf = 1.952 $\chi^2 = 4738.99$ $P < .001$	Edf = 1.880 $\chi^2 = 53.57$ $P < .001$	Edf = 1.772 $\chi^2 = 169.43$ $P < .001$	Edf = 6.520 $\chi^2 = 164.71$ $P < .001$
Energetic Density	36.7%	1609.741	Edf = 0.9783 $\chi^2 = 107.31$ $P < .001$	Edf = 1.5508 $\chi^2 = 2533.33$ $P < .001$	Edf = 0.9538 $\chi^2 = 39.49$ $P < .001$	Edf = 1.4011 $\chi^2 = 3180.73$ $P < .001$	Edf = 6.5223 $\chi^2 = 162.30$ $P < .001$
NASC	36.3%	1624.153	Edf = 1.248 $\chi^2 = 142.73$ $P < .001$	Edf = 1.778 $\chi^2 = 1930.5$ $P < .001$	Edf = 0.946 $\chi^2 = 20.71$ $P < .001$	Edf = 1.710 $\chi^2 = 491.08$ $P < .001$	Edf = 6.525 $\chi^2 = 172.99$ $P < .001$
Proportion *T. spinifera*	40.8%	1514.347	Edf = 1.9366 $\chi^2 = 315.3$ $P < .001$	Edf = 0.9827 $\chi^2 = 437.4$ $P < .001$	Edf = 1.8670 $\chi^2 = 87.7$ $P = .177$	Edf = 0.9852 $\chi^2 = 762.8$ $P < .001$	Edf = 6.5492 $\chi^2 = 139.8$ $P < .001$
Biomass CPUE	36.4%	1614.378	Edf = 1.356 $\chi^2 = 85.0$, $P < .001$	Edf = 1.376 $\chi^2 = 3172.0$ $P < .001$	Edf = 1.185 $\chi^2 = 406.0$ $P < .001$	Edf = 1.868 $\chi^2 = 148.1$ $P < .001$	Edf = 6.534 $\chi^2 = 144.7$ $P < .001$

For each model, we report deviance explained and AIC. For each smooth interaction term (e.g. early season—offshore, late season—onshore, etc.) and the random effect (survey), we report estimated degrees of freedom (edf), χ^2, and *P* values. Krill NASC (Nautical Area Scattering Coefficient, m^2 nmi^{-2}) is a relative abundance metric, and biomass CPUE is catch per unit effort (kg krill/km observation effort).

the shelf break and *E. pacifica* offshore (Fig. S3). For both species, length varied seasonally and spatially (Table 2) with the largest *T. spinifera* observed in the offshore-south ecoregion during the early season (Fig. 2).

Krill caloric content was not explained by spatial distribution within the ecoregions or by sex, but it did vary significantly based on species and season (Fig. 3), and reproductive status (Table 2). *E. pacifica* and *T. spinifera* caloric contents were not significantly different during the early foraging season (median = 2.79 kJ g^{-1} WW and 2.86 kJ g^{-1} WW, respectively), but they differed in the late foraging season (3.73 kJ g^{-1} WW and 5.85 kJ g^{-1} WW, respectively). Reproductive individuals of both species and sexes had significantly lower caloric contents than those without attached spermatophores (Table 2). Length was a significant predictor of caloric content for *T. spinifera* in the late season and *E. pacifica* during both seasons ($P < .001$; Fig. 4). Swarm energetic density varied seasonally and spatially (Table 2), with

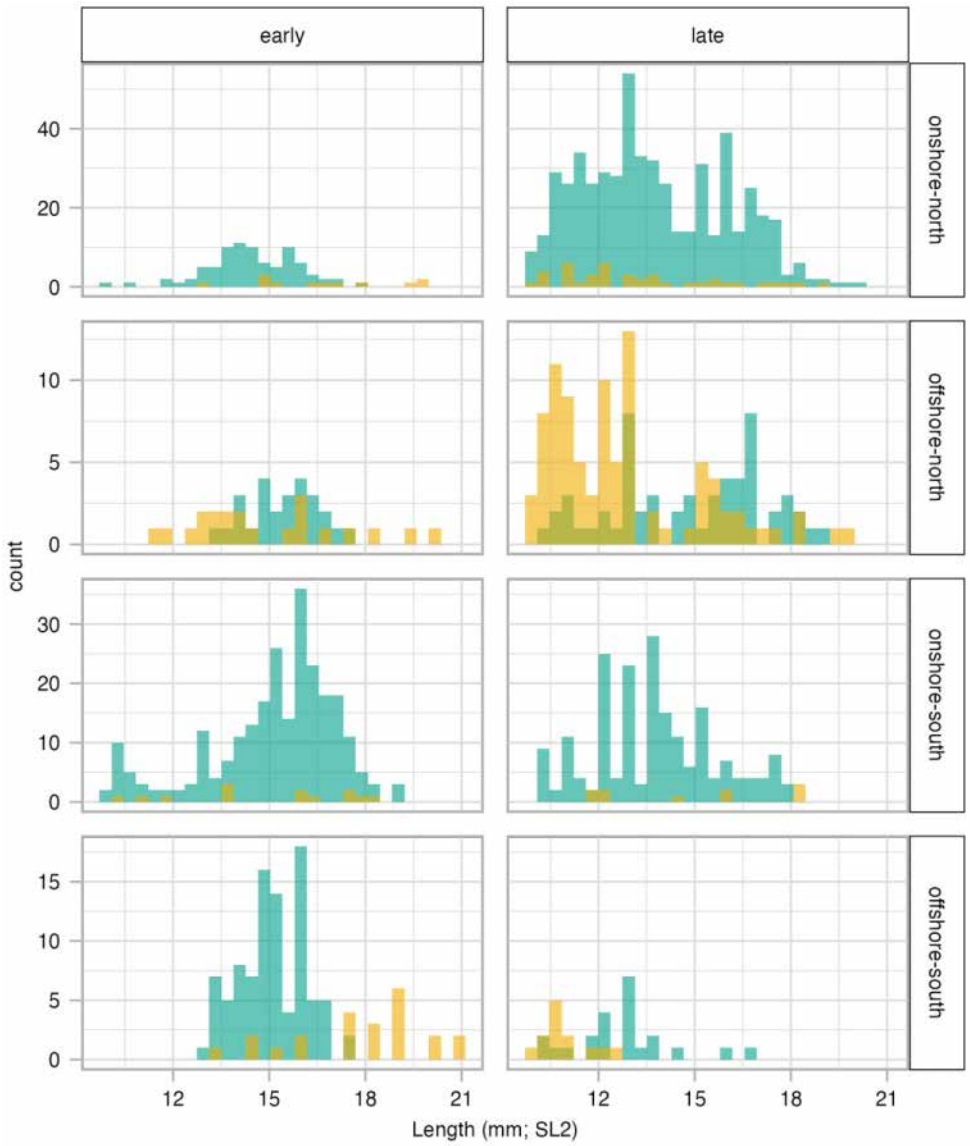

Figure 2. Krill (green: *E. pacifica*; yellow: *T. spinifera*) length frequency distribution in each ecoregion (onshore-north, offshore-north, onshore-south, and offshore-south) and humpback whale foraging season (early: March–June and late: July–November).

significantly higher values in the late season and onshore (medians = 28 kilojoules/m^3) than in the early season or offshore (medians = 27 kilojoules/m^3).

We observed 76 humpback whale groups, containing between 1 and 4 individuals, across all surveys (early season: *n* groups = 39, late season: *n* groups = 37; continental shelf: *n* groups = 50, offshore: *n* groups = 26). The proportion of *T. spinifera* in the 5 km areas around sighted whales varied seasonally and in a seasonal-spatial interaction, with a higher fraction of *T. spinifera* near whales (onshore median = 0.30, offshore median = 0.28; Fig. S4) compared to background points (onshore and offshore median = 0). This relationship was more pronounced in the late foraging season (whale sighting area median = 0.51; background point median = 0) than the early season (whale sighting area median = 0.28; background point median = 0).

Biomass of krill swarms (n = 2242) ranged from 0.48 to 2.46 × 10^9 kg and varied significantly based on cross-shelf distribution (Table 2). Biomass was greater offshore (median = 1140 kg; n = 1,421 swarms) compared to onshore (median = 510 kg; n = 821 swarms), and swarms were deeper offshore (median depth = 182 m) compared to onshore (median depth = 106 m). Similarly, swarm biomass CPUE in the 5 km areas around each whale varied significantly based on cross-shelf distribution and season (onshore median = 0.020 kg/km; offshore median = 54.4 kg/km; early season median = 0.026 kg/km; and late season = 1.19 kg/km), and values were elevated above background points (all medians = 0 kg/km). Higher values of all prey metrics tended to be associated with areas of humpback whale presence rather than background points (Fig. S4).

Humpback whale–krill models

In five GAMs modeling binomial humpback whale presence/pseudo-absence (Fig. 5), relationships with krill

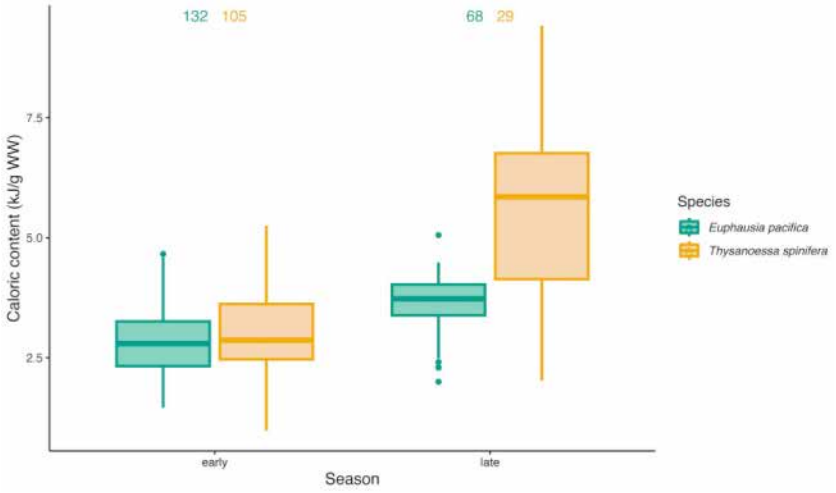

Figure 3. Mass-specific caloric content (kilojoules per gram wet weight; kJ g^{-1} WW) of krill species in the early (March–June) and late (July–November) foraging seasons. Boxplot—dark line: median; box: interquartile range (IQR); error bars: max/min within 1.5 × IQR above/below IQR; and dots: outliers.

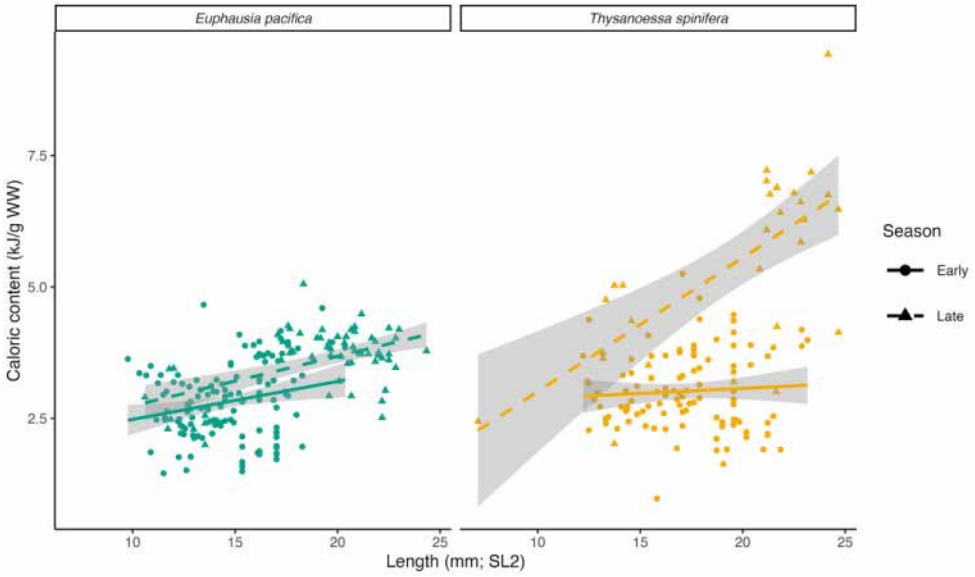

Figure 4. Seasonal and species-specific relationships between krill length (mm) and mass-specific caloric content (kilojoules per gram wet weight; kJ g^{-1} WW). Dots and solid trend lines: early humpback whale foraging season; triangles and dashed trend lines: late foraging season. Smooths are fitted by linear regression (*E. pacifica* r^2-adjusted = 0.31, *T. spinifera* r^2-adjusted = 0.61), with 95% confidence intervals in gray. Length was a significant predictor of caloric content for *T. spinifera* in the late season and *E. pacifica* during both seasons ($P < .001$).

prey metrics varied seasonally and spatially. Apart from the early season onshore term in the Proportion *T. spinifera* Model, all model terms were significant ($P < .001$; Table 3). In the NASC Model (deviance explained = 36.3%), the partial effect on whale presence was greatest offshore during the early foraging season (Fig. 5a). During the late foraging season, the partial effect of offshore krill NASC was lower than that onshore, where log NASC ∈ [0, 5], when the relationship reversed (Fig. 5b). Similarly, the Swarm Biomass Model (deviance explained = 40.7%), which contextualized how much biomass was available within the immediate foraging environment, showed a positive relationship between whale presence and increasing biomass, particularly onshore in the early season (Fig. 5c) and offshore in the late season (Fig. 5d). In the Biomass CPUE Model (deviance explained = 36.4%), which captured the patchiness of the foraging environment, the partial effect onshore was linear in the early season (Fig. 5e), while the offshore trend declined following a midrange peak, and the relationship reversed in the late season (Fig. 5f). The Energetic Density Model (deviance explained = 36.7%) showed a greater effect on whale presence offshore in the early season (Fig. 5g) and linear relationships both onshore and offshore in the late season (Fig. 5h). In the Proportion *T. spinifera* Model (deviance explained = 40.8%), spatial relationships were linear and uniform in the late season (Fig. 5j), whereas in the early season, the offshore term had a greater effect at higher values, and the onshore partial effect decreased to become negative at high values (Fig. 5i).

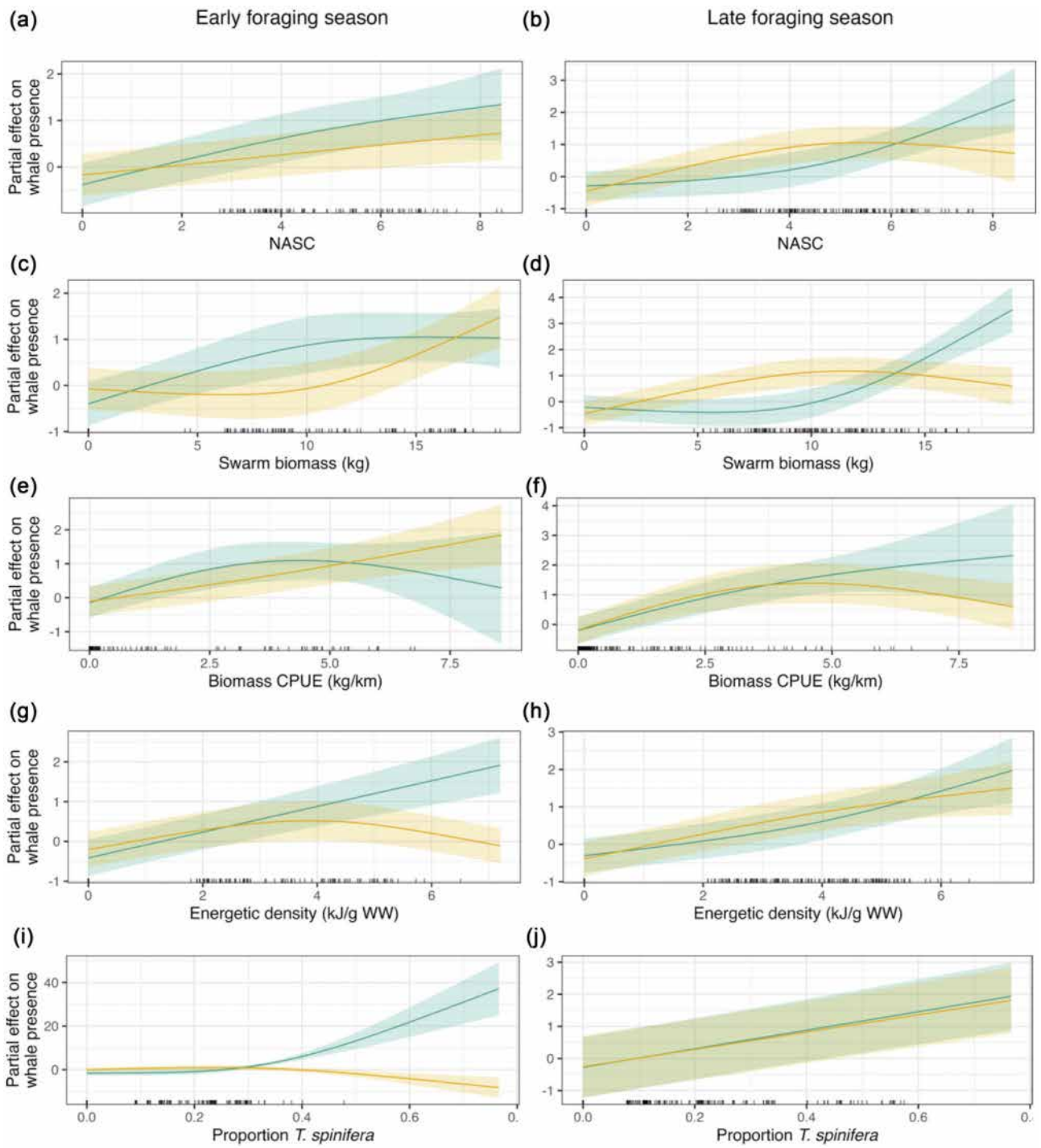

Figure 5. Humpback whale–krill relationships from generalized additive models across time (early versus late foraging season) and space (continental shelf versus offshore). Response curves represent the effect of the smooth function upon the trend in humpback whale presence, with higher values indicating higher predicted probability of occurrence. Prey metrics (in descending order) are logged swarm biomass (kg), logged swarm NASC (Nautical Area Scattering Coefficient; m^2 nmi^{-2}), logged biomass CPUE (catch per unit effort; kg/km observation effort), logged energetic density (kilojoules/m^3), and proportion *T. spinifera*. Shaded ribbons: 95% confidence intervals, colored per fitted trend (orange: continental shelf; blue: offshore). Green indicates overlap between the regional response curves.

Discussion

We found that humpback whale presence in the NCC relates to diverse metrics of krill swarm quality and quantity, including energetic density, species composition, and biomass. Overall, increases in these metrics were positively related to humpback whale presence, with increasing trends modified by seasonal (early versus late foraging season) and spatial (on the continental shelf versus offshore) variation. These results suggest that humpback whales select preyscape areas that offer both plentiful and high-quality krill. Understanding variability in krill prey metrics in space and time, and with regard to

humpback whale presence can inform future studies linking baleen whale predators and krill, such as species distribution modeling efforts.

Spatiotemporal dynamics of krill preyscape quality

Our study found spatiotemporal variability in krill energetic quality available to foraging humpback whales. Latitude was not a significant predictor of distribution for either krill species, suggesting a relatively even alongshore distribution across large scales of the NCC. In contrast, distance from the shelf break was a strong predictor of species-specific krill distributions, with *E. pacifica* concentrated along and offshore of the shelf break and *T. spinifera* inshore of the shelf break, supporting previous work in the region (Gómez-Gutiérrez et al. 2005, Lindsey and Batchelder 2011, Derville et al. 2024). These cross-shelf patterns likely drive distributions of whales and other krill predators, many of which tend to occupy the shelf break where krill are abundant (Derville et al. 2022). Individual krill swarms had higher biomass offshore than on the continental shelf, offering an important resource for foraging baleen whales that require high prey biomass. However, offshore swarms were deeper than those on the shelf, potentially requiring higher energetic expenditure to capture the deeper prey.

Krill caloric content was comparable between species in the early foraging season (March–June) and significantly elevated, particularly for *T. spinifera*, in the late season (July–November). Mature individuals of both krill species with spermatophores present had lower caloric contents than those without, echoing patterns in lipid content (Fisher et al. 2020). The late-season differences in caloric content may result from life history strategies utilized by the two krill species. *Thysanoessa spinifera* does not allocate energy to reproduction at the expense of growth, while *E. pacifica* allocates more energy to reproduction, shows negative growth, and has consistently lower lipid levels (Feinberg and Peterson 2003, Ju et al. 2009, Fisher et al. 2020). During the late foraging season, following several months of upwelling conditions, *T. spinifera* exhibited a greater degree of variability in caloric content than *E. pacifica*, which may reflect the quality of phytoplankton in a given year. Differences in life history strategies between these two sympatric krill species may shape their tolerance of environmental conditions, drive species-specific responses to extreme events and climate change forcing (Weber et al. 2021), and mediate the energy available to whales (Fiechter et al. 2020).

Interestingly, we found that *E. pacifica* individuals had higher mass-specific caloric content with increased length, as did *T. spinifera* in the late foraging season. Baleen whale species target specific krill length classes in Antarctica (Santora et al. 2010), and targeting larger krill in colder waters may be advantageous for blue whales and drive the timing of their arrival on the NCC foraging grounds (Szesciorka et al. 2020). In the NCC, krill length varies relative to environmental conditions, including temperature and chlorophyll [T. Shaw and J. Fisher (personal communication)], and as a result of physical circulation and advection processes (Lindsey and Batchelder 2011, Fiechter et al. 2020).

Fine-scale humpback whale–krill relationships

The Marginal Value Theorem predicts foraging animals should pursue only prey patches in which the energy intake rate exceeds that of the average surrounding environment (Charnov 1976), a result of the interplay between available prey species, biomass, and energetic density. At the 5 km spatial scale used in this study, relationships with important prey metrics allowed us to assess humpback whale selection of krill quality (energetic density), quantity (biomass), and species composition, all in comparison to average values of these metrics in the background preyscape. Although we could not model variables together due to high correlation, our single metric model approach allowed us to assess and compare two biomass metrics (mean swarm biomass and biomass CPUE, a measure of prey patchiness) as well as the average swarm energetic density and proportion of *T. spinifera* available to humpback whales. Additionally, this approach enabled us to test a common acoustic proxy for krill abundance, NASC, in comparison to the more analytically complex metric of swarm biomass. All models showed good performance, with deviance explained values greater than 36%. The best models indicated that the proportion of *T. spinifera* in a swarm, swarm biomass, and energetic density were the most important factors explaining humpback whale presence.

Krill swarm energetic density had a positive effect on humpback whale occurrence, particularly in the late season when *T. spinifera* and *E. pacifica* have significantly different caloric contents, suggesting humpback whales target higher-quality swarms that offer more energy per lunge. However, this positive relationship was not present onshore during the early season, when the two krill species had similar caloric content. Humpback whales also target forage fish on the continental shelf (Santora et al. 2020) that have higher energetic densities than krill (Price et al. 2024), indicating that whales may selectively forage on fish despite higher energetic costs to capture them (Chenoweth et al. 2021). Variation in seasonal and spatial relationships with krill swarm energetic density may explain why humpback whales prey-switch. Fish are likely more energetically advantageous onshore during the early season, and krill are more energetically advantageous during the late season and offshore during both seasons.

Swarm biomass was assessed based on the average biomass of krill swarms within 5 km of sighted whales, and our results emphasize the value of high-biomass swarms in explaining humpback whale presence. The Biomass CPUE Model, which captures the patchiness of the foraging environment, had lower explanatory capacity. Interestingly, the effects of these variables on sighted whale groups were distinct. For example, in the early season, the partial effect of swarm biomass on humpback whale presence increased steeply onshore and was flatter offshore. This trend reversed in the late season, with a steep increase offshore and flatter onshore trend. This variability may reflect the foraging flexibility of humpback whales, which allows them to navigate tradeoffs between prey quality and quantity. In the late season offshore, krill quality (elevated due to higher late season caloric contents) together with quantity (higher offshore biomass) may make offshore swarms more favorable for the whales, despite being deeper.

Across all models, several trends were characterized by midrange peaks followed by slight negative relationships at high values, which may indicate that model predictions are less certain at data extremes and with low observation density (Wood 2017). These results may also represent the functional response of humpback whales to very high biomass patches or the generalist feeding strategies they utilize, including prey-switching to target prey based on availability and quality.

Foraging lunges are relatively inexpensive (Videsen et al. 2023), and humpback whales do not need to exploit only the densest aggregations in order to break even energetically (Hazen et al. 2009). Flatter trends and seasonal and spatial variability in our models may suggest humpback whales target krill swarms that meet a threshold of profitability, rather than seeking only the highest-quality swarms, or that humpback whales, as a low-prevalence species, cannot occupy all the best areas of the NCC foraging grounds simultaneously. While our methodological approach collected a snapshot of whale and prey distribution on the foraging grounds, it cannot resolve behavioral state, and some whale groups in this study assumed to be foraging may have been traveling or engaging in other nonfeeding behaviors less associated with the krill metrics evaluated. In Antarctica, humpback whale feeding rates are highest immediately after the annual fasting period, and their feeding behaviors change throughout the foraging season (Nichols et al. 2022). Humpback whales in the NCC may likewise tune their foraging efforts relative to life history demands like migration and fasting.

Positive relationships between the proportion of *T. spinifera* in a krill swarm and humpback whale presence suggest this species preferentially preys upon *T. spinifera*, particularly during the late foraging season, similarly to blue whales (Fiedler et al. 1998), multiple species of seabirds (Santora et al. 2011), and fish (Tanasichuk 1998a). Modeled relationships were much weaker in the early season, and while the offshore trend became positive at high proportions of *T. spinifera* (though there were relatively few observations), onshore relationships became negative at the highest concentrations of *T. spinifera*. This may indicate that when *E. pacifica* and *T. spinifera* have the same weight-standardized caloric content (as in the early season), targeting *T. spinifera* does not confer an advantage to humpback whales, and they may prey-switch to forage fish. In contrast, higher proportions of *T. spinifera* in the late season were associated with higher humpback whale presence. These relationships suggest humpback whales target *T. spinifera*, particularly in the late season when they are energetically richer than *E. pacifica*.

In addition to testing prey quality metrics, the NASC model assessed a methodological question: what explanatory power is gained by calculating biomass rather than using relative abundance, which is commonly used in whale-prey studies (e.g. Hazen et al. 2009, Santora et al. 2020)? While the species, season, and spatially informed biomass calculations we generated did provide additional information and explanatory capacity, the comparable performance of the NASC Model suggests relative abundance is a reliable proxy for biomass. This can be advantageous, as measuring NASC is a less data- and computationally-intensive metric. Interestingly, one of our best-performing models, based on only the proportion of *T. spinifera* in swarms, is also one of our most accessible variables, as krill species distribution models have successfully predicted *T. spinifera* in the NCC (Derville et al. 2024). Integrating these two relatively simple metrics could support predictions of humpback whale distributions and inform future whale-prey studies.

Future implications

Variability in krill prey quality and relationships with humpback whale distributions may exemplify how oceanographic processes like upwelling, mediated through prey and trophic relationships, impact baleen whales (Ryan et al. 2022, Price et al. 2024). Environmental conditions are changing in the NCC, with events like marine heatwaves and strong El Niño events influencing and potentially decoupling key phenological processes (Asch 2015, Jorgensen et al. 2024), leading to nonstationarity of ecological relationships and distributional shifts across marine taxa (Muhling et al. 2020). *E. pacifica* and *T. spinifera* may respond to climate forcing differently based on their life history strategies (Tanasichuk 1998a, 1998b, Ju et al. 2009). Physiological changes, such as the association between smaller *E. pacifica* and warmer waters (Robertson and Bjorkstedt 2020), could lead to decreased krill energetic density (Price et al. 2024) available for predators. Further, distributional shifts, including the disappearance of *T. spinifera* from the NCC during the 2014–2015 NE Pacific marine heatwave (Peterson et al. 2017), could diminish or remove this key prey item. As a result of climate and environmental changes, humpback whales may encounter lower-quality prey and/or spatiotemporal distribution shifts (Fleming et al. 2016, Cheeseman et al. 2024), potentially leading to increased overlap with fishing gear that can result in entanglement (Santora et al. 2020). Clearer understanding of humpback whale–krill relationships, including prey patch selection with regards to energetic density, biomass, and species composition, can improve species distribution models and aid resource managers in mitigating entanglement risk on the NCC foraging grounds (Derville et al. 2023).

In addition to studying relationships between whales and the quantity and distribution of their prey, clarifying the influence of prey quality on whale distributions offers a valuable opportunity for improved spatial management in the NCC and beyond. Climate change and human use of the ocean present threats to whales and other marine wildlife, including changing environmental conditions, ship strikes, and entanglement events common in this region and globally. Our findings and approach can be used to elucidate predator–prey relationships in other marine ecosystems. Quantifying prey quality and variation in distributions may enable predictions of predator distributions, offering another tool for conservation management.

Acknowledgments

We thank the NOAA Northwest Fisheries Science Center and the crew and science parties of the R/V *Bell M. Shimada* for facilitating data collection; A. Nodal and T. Davis for collecting krill at sea; R. Albertson, D. Barlow, C. Bird, A. Kownacki, and F. Sullivan for marine mammal observation; and O. Burnip, A. Kent, H. Robinson, and A. Tomita for processing krill samples. An AI resource (ChatGPT) was used to troubleshoot coding problems.

Author contributions

L.T., K.B., and S.D. acquired funding and conceptualized the project; E.P., S.D, and J.W. provided guidance and oversight on methodology and analysis; J.F. and E.D. collected, processed, and analyzed data and provided guidance on analysis; R.K. collected and processed data, conducted data analysis, and wrote the manuscript; all authors critically reviewed the manuscript. All authors contributed to the article and approved the submitted version.

Supplementary data

Supplementary data is available at *ICES Journal of Marine Science* online.

Conflict of interest: None declared.

Funding

This research received financial support from the NOAA Species Recovery Grant (#NA19NMF4720109), the Oregon State University Marine Mammal Institute, the Oregon Department of Fish & Wildlife (ODFW), Oregon Sea Grant, and the NSF Graduate Research Fellowship Program.

Data availability

The data underlying this article are available via the Figshare Digital Repository: https://figshare.com/projects/OPAL_Overlap_Predictions_About_Large_whales/161137

References

Asch RG. Climate change and decadal shifts in the phenology of larval fishes in the California Current ecosystem. *Proc Natl Acad Sci* 2015;**112**:E4065–74. https://doi.org/10.1073/pnas.1421946112

Benoit-Bird KJ. Resource patchiness as a resolution to the food paradox in the sea. *Am Nat* 2024;**203**:1–13. https://doi.org/10.1086/727473

Brinton E. The distribution of the Pacific euphausiids. *Bull Scripps Inst Oceanogr* 1962;**8**:21–270.

Brinton E. Vertical migration and avoidance capability of euphausiids in the California current: vertical migration and avoidance capability of euphausiids. *Limnol Oceanogr* 1967;**12**:451–83. https://doi.org/10.4319/lo.1967.12.3.0451

Buckland ST, Rexstad EA, Marques TA *et al. Distance Sampling: Methods and Applications. Methods in Statistical Ecology*. Cham: Springer International Publishing, 2015.

Cade DE, Kahane-Rapport SR, Wallis B *et al.* Evidence for size-selective predation by Antarctic humpback whales. *Front Mar Sci* 2022;**9**:747788. https://doi.org/10.3389/fmars.2022.747788

Charnov EL. Optimal foraging: the marginal value theorem. *Theor Popul Biol* 1976;**9**:129–36. https://doi.org/10.1016/0040-5809(76)90040-X

Checkley DM, Barth JA. Patterns and processes in the California Current System. *Prog Oceanogr* 2009;**83**:49–64. https://doi.org/10.1016/j.pocean.2009.07.028

Cheeseman T, Barlow J, Acebes JM *et al.* Bellwethers of change: population modelling of North Pacific humpback whales from 2002 through 2021 reveals shift from recovery to climate response. *R Soc Open Sci* 2024;**11**:231462. https://doi.org/10.1098/rsos.231462

Chenoweth E, Boswell K, Friedlaender A *et al.* Confronting assumptions about prey selection by lunge-feeding whales using a process-based model. *Funct Ecol* 2021;**35**:1722–34. https://doi.org/10.1111/1365-2435.13852

Conover WJ, Iman RL. Rank transformations as a bridge between parametric and nonparametric statistics. *Am Stat* 1981;**35**:124–9. https://doi.org/10.1080/00031305.1981.10479327

Cotté C, d'Ovidio F, Chaigneau A *et al.* Scale-dependent interactions of Mediterranean whales with marine dynamics. *Limnol Oceanogr* 2011;**56**:219–32. https://doi.org/10.4319/lo.2011.56.1.0219

Derville S, Barlow DR, Hayslip C *et al.* Seasonal, annual, and decadal distribution of three rorqual whale species relative to dynamic ocean conditions off Oregon. *USA Front Mar Sci* 2022;**9**:868566.

Derville S, Buell TV, Corbett KC *et al.* Exposure of whales to entanglement risk in Dungeness crab fishing gear in Oregon, USA, reveals distinctive spatio-temporal and climatic patterns. *Biol Conserv* 2023;**281**:109989. https://doi.org/10.1016/j.biocon.2023.109989

Derville S, Fisher JL, Kaplan RL *et al.* A predictive krill distribution model for *Euphausia pacifica* and *Thysanoessa spinifera* using scaled acoustic backscatter in the Northern California Current. *Prog Oceanogr* 2024;**231**:103388.

Doniol-Valcroze T, Lesage V, Giard J *et al.* Optimal foraging theory predicts diving and feeding strategies of the largest marine predator. *Behav Ecol* 2011;**22**:880–8. https://doi.org/10.1093/beheco/arr038

Dorman JG, Sydeman WJ, Thompson SA *et al.* Environmental variability and krill abundance in the central California current: implications for ecosystem monitoring. *Front Mar Sci* 2023;**10**:1099482. https://doi.org/10.3389/fmars.2023.1099482

Dormann CF, Elith J, Bacher S *et al.* Collinearity: a review of methods to deal with it and a simulation study evaluating their performance. *Ecography* 2013;**36**:27–46. https://doi.org/10.1111/j.1600-0587.2012.07348.x

Färber-Lorda J, Beier E, Mayzaud P. Morphological and biochemical differentiation in Antarctic krill. *J Mar Syst* 2009;**78**:525–35. https://doi.org/10.1016/j.jmarsys.2008.12.022

Feinberg LR, Peterson WT. Variability in duration and intensity of euphausiid spawning off central Oregon, 1996–2001. *Prog Oceanogr* 2003;**57**:363–79. https://doi.org/10.1016/S0079-6611(03)00106-X

Fiechter J, Santora JA, Chavez F *et al.* Krill hotspot formation and phenology in the California current ecosystem. *Geophys Res Lett* 2020;**47**. https://doi.org/10.1029/2020GL088039

Fiedler PC, Reilly SB, Hewitt RP *et al.* Blue whale habitat and prey in the California Channel Islands. *Deep Sea Res Part II* 1998;**45**:1781–801. https://doi.org/10.1016/S0967-0645(98)80017-9

Fisher JL, Menkel J, Copeman L *et al.* Comparison of condition metrics and lipid content between *Euphausia pacifica* and *Thysanoessa spinifera* in the northern California Current, USA. *Prog Oceanogr* 2020;**188**:102417.

Fleming AH, Clark CT, Calambokidis J *et al.* Humpback whale diets respond to variance in ocean climate and ecosystem conditions in the California Current. *Glob Chang Biol* 2016;**22**:1214–24. https://doi.org/10.1111/gcb.13171

Fossette S, Abrahms B, Hazen EL *et al.* Resource partitioning facilitates coexistence in sympatric cetaceans in the California Current. *Ecol Evol* 2017;**7**:9085–97. https://doi.org/10.1002/ece3.3409

Goldbogen JA, Hazen EL, Friedlaender AS *et al.* Prey density and distribution drive the three-dimensional foraging strategies of the largest filter feeder. *Funct Ecol* 2015;**29**:951–61. https://doi.org/10.1111/1365-2435.12395

Gómez-Gutiérrez J, Peterson WT, Miller CB. Cross-shelf life-stage segregation and community structure of the euphausiids off central Oregon (1970–1972). *Deep Sea Res Part II* 2005;**52**:289–315. https://doi.org/10.1016/j.dsr2.2004.09.023

Hazen E, Friedlaender A, Thompson M *et al.* Fine-scale prey aggregations and foraging ecology of humpback whales megaptera novaeangliae. *Mar Ecol Prog Ser* 2009;**395**:75–89. https://doi.org/10.3354/meps08108

Jarvis T, Kelly N, Kawaguchi S *et al.* Acoustic characterisation of the broad-scale distribution and abundance of Antarctic krill (*Euphausia superba*) off East Antarctica (30–80°E) in January–March 2006. *Deep Sea Res Part II* 2010;**57**:916–33. https://doi.org/10.1016/j.dsr2.2008.06.013

Jönsson KI. Capital and income breeding as alternative tactics of resource use in reproduction. *Oikos* 1997;**78**:57–66. https://doi.org/10.2307/3545800

Jorgensen EM, Hazen EL, Jacox MG *et al.* Physical and biogeochemical phenology of coastal upwelling in the California Current System. *Geophys Res Lett* 2024;**51**:e2024GL108194. https://doi.org/10.1029/2024GL108194

Ju S-J, Kang H-K, Kim WS *et al.* Comparative lipid dynamics of euphausiids from the Antarctic and Northeast Pacific Oceans. *Mar Biol* 2009;**156**:1459–73. https://doi.org/10.1007/s00227-009-1186-1

Kaplan R, Derville S, Bernard K *et al.* Humpback-krill relationships are strongest at fine spatial scales in the Northern California Current

region. *Mar Ecol Prog Ser* 2024;**729**:219–32. https://doi.org/10.3354/meps14510
Lindsey BJ, Batchelder HP. Cross-shelf distribution of *Euphausia pacifica* in the Oregon coastal upwelling zone: field evaluation of a differential transport hypothesis. *J Plankton Res* 2011;**33**:1666–78. https://doi.org/10.1093/plankt/fbr073
Marra G, Wood SN. Practical variable selection for generalized additive models. *Comput Stat Data Anal* 2011;**55**:2372–87. https://doi.org/10.1016/j.csda.2011.02.004
Mauchline J. The biology of Mysids and Euphausiids. *Adv Mar Biol* 1980;**18**:1677.
Miller EJ, Potts JM, Cox MJ *et al.* The characteristics of krill swarms in relation to aggregating Antarctic blue whales. *Sci Rep* 2019;**9**:16487. https://doi.org/10.1038/s41598-019-52792-4
Mizroch S, Rice D, Zwiefelhofer D *et al.* Distribution and movements of fin whales in the North Pacific Ocean. *Mammal Rev* 2009;**39**:193–227. https://doi.org/10.1111/j.1365-2907.2009.00147.x
Muhling BA, Brodie S, Smith JA *et al.* Predictability of species distributions deteriorates under novel environmental conditions in the California Current System. *Front Mar Sci* 2020;**7**. https://doi.org/10.3389/fmars.2020.00589
Murdoch WW. Switching in general predators: experiments on predator specificity and stability of prey populations. *Ecol Monog* 1969;**39**:335–54. https://doi.org/10.2307/1942352
Nichols RC, Cade DE, Kahane-Rapport S *et al.* Intra-seasonal variation in feeding rates and diel foraging behaviour in a seasonally fasting mammal, the humpback whale. *R Soc Open Sci* 2022;**9**:211674. https://doi.org/10.1098/rsos.211674
Nickels CF, Sala LM, Ohman MD. The morphology of euphausiid mandibles used to assess selective predation by blue whales in the southern sector of the California Current System. *J. Crustacean Biol*, 2018;**38**:563–73. https://doi.org/10.1093/jcbiol/ruy062
Pebesma E, Bivand R. *Spatial Data Science: With Applications in R*. London: Chapman and Hall/CRC, 2023.
Peterson WT, Fisher JL, Strub PT *et al.* The pelagic ecosystem in the Northern California Current off Oregon during the 2014–2016 warm anomalies within the context of the past 20 years. *J Geophys Res: Oceans* 2017;**122**:7267–90. https://doi.org/10.1002/2017JC012952
Phillips EM, Chu D, Gauthier S *et al.* Spatiotemporal variability of euphausiids in the California Current Ecosystem: insights from a recently developed time series. *ICES J Mar Sci* 2022;**79**:1312–26. https://doi.org/10.1093/icesjms/fsac055
Price SE, Savoca MS, Kumar M *et al.* Energy densities of key prey species in the California Current ecosystem. *Front Mar Sci* 2024;**10**:1345525. https://doi.org/10.3389/fmars.2023.1345525
R Core Team. *R: A Language and Environment for Statistical Computing*. Vienna: R Foundation for Statistical Computing, 2024. https://www.R-project.org/
Robertson RR, Bjorkstedt EP. Climate-driven variability in *Euphausia pacifica* size distributions off northern California. *Prog Oceanogr* 2020;**188**:102412. https://doi.org/10.1016/j.pocean.2020.102412
Ryan JP, Benoit-Bird KJ, Oestreich WK *et al.* Oceanic giants dance to atmospheric rhythms: ephemeral wind-driven resource tracking by blue whales. *Ecol Lett* 2022;**25**:2435–47. https://doi.org/10.1111/ele.14116
Santora J, Reiss C, Loeb V *et al.* Spatial association between hotspots of baleen whales and demographic patterns of Antarctic krill euphausia superba suggests size-dependent predation. *Mar Ecol Prog Ser* 2010;**405**:255–69. https://doi.org/10.3354/meps08513
Santora JA, Mantua NJ, Schroeder ID *et al.* Habitat compression and ecosystem shifts as potential links between marine heatwave and record whale entanglements. *Nat Commun* 2020;**11**:536. https://doi.org/10.1038/s41467-019-14215-w
Santora JA, Ralston S, Sydeman WJ. Spatial organization of krill and seabirds in the central California Current. *ICES J Mar Sci* 2011;**68**:1391–402. https://doi.org/10.1093/icesjms/fsr046
Spitz J, Trites AW, Becquet V *et al.* Cost of living dictates what whales, Dolphins and porpoises eat: the importance of prey quality on predator foraging strategies. *PLoS One* 2012;**7**:e50096. https://doi.org/10.1371/journal.pone.0050096
Szesciorka AR, Ballance LT, Širović A *et al.* Timing is everything: drivers of interannual variability in blue whale migration. *Sci Rep* 2020;**10**:7710. https://doi.org/10.1038/s41598-020-64855-y
Tanasichuk R. Interannual variations in the population biology and productivity of *Thysanoessa spinifera* in Barkley Sound, Canada, with special reference to the 1992 and 1993 warm ocean years. *Mar Ecol Prog Ser* 1998a;**173**:181–95. https://doi.org/10.3354/meps173181
Tanasichuk RW. Interannual variations in the population biology and productivity of *Euphausia pacifica* in Barkley Sound, Canada, with special reference to the 1992 and 1993 warm ocean years. *Mar Ecol Prog Ser* 1998b;**173**:163–80. https://doi.org/10.3354/meps173163
Videsen SKA, Simon M, Christiansen F *et al.* Cheap gulp foraging of a giga-predator enables efficient exploitation of sparse prey. *Sci Adv* 2023;**9**:eade3889. https://doi.org/10.1126/sciadv.ade3889
Weber ED, Auth TD, Baumann-Pickering S *et al.* State of the California current 2019–2020: back to the future with marine heatwaves? *Front Mar Sci* 2021;**8**. https://doi.org/10.3389/fmars.2021.709454
Wei T, Simko V. *R package 'corrplot': visualization of a correlation matrix*. 2024. https://github.com/taiyun/corrplot (last accessed: December 6, 2024)
Wood SN. Fast stable restricted maximum likelihood and marginal likelihood estimation of semiparametric generalized linear models. *J R Stat Soc., B: Stat Methodol* 2011;**73**:3–36. https://doi.org/10.1111/j.1467-9868.2010.00749.x
Wood SN. *Generalized Additive Models: An Introduction with R*. London: Chapman and Hall/CRC, 2017, 496.

Handling Editor: Richard O'Driscoll